Selectivity, efficacy and toxicity studies of UCCB01-144, a dimeric neuroprotective PSD-95 inhibitor

Selectivity, efficacy and toxicity studies of UCCB01-144, a dimeric neuroprotective PSD-95 inhibitor

Anders Bach[a, 1], Bettina H. Clausen[b, c, 1], Lotte K. Kristensen[d, 2], Maria G. Andersen[b, 3], Ditte Gry Ellman[b], Pernille B. L. Hansen[e, 4], Henrik Hasseldam[d], Marc Heitz[a, 5], Dennis Özcelik[a], Ellie J. Tuck[f, 6], Maksym V. Kopanitsa[f, 7], Seth G. N. Grant[g], Karin Lykke-Hartmann[h], Flemming F. Johansen[d], Kate L. Lambertsen[b, c, i, 8], Kristian Strømgaard[a, 8]

[a]Department of Drug Design and Pharmacology, University of Copenhagen, Copenhagen, Denmark.
[b]Department of Neurobiology Research, Institute of Molecular Medicine, University of Southern Denmark, Odense, Denmark.
[c]BRIDGE - Brain Research - Inter-Disciplinary Guided Excellence, Department of Clinical Research, University of Southern Denmark, Odense, Denmark.
[d]Molecular Pathology Section, BRIC, Copenhagen Biocenter, University of Copenhagen, Copenhagen, Denmark.
[e]Department of Cardiovascular and Renal Research, Institute of Molecular Medicine, University of Southern Denmark, Odense, Denmark.
[f]Synome Ltd, Babraham Research Campus, Cambridge, United Kingdom
[g]Centre for Clinical Brain Sciences, University of Edinburgh, Edinburgh, United Kingdom
[h]Department of Biomedicine and Department of Clinical Medicine, University of Aarhus, Aarhus, Denmark and and the Department of Clinical Genetics, Aarhus University Hospital, Aarhus, Denmark.
[i]Department of Neurology, Odense University Hospital, Odense, Denmark

[1]These authors contributed equally to this work as first authors
[2]Present address: Minerva Imaging, Copenhagen, Denmark; and Department of Clinical Physiology, Nuclear Medicine & PET and Cluster for Molecular Imaging, Department of Biomedical Sciences, Rigshospitalet and University of Copenhagen, Denmark
[3]Present address: ALK-Abelló A/S, Hørsholm, Denmark
[4]Present address: Cardiovascular, Renal and Metabolic, IMED Biotech Unit, AstraZeneca, Gothenburg, Sweden
[5]Present address: Department of Chemistry and Biochemistry, University of Bern, Bern, Switzerland
[6]Present address: The Gurdon Institute, University of Cambridge, Cambridge, United Kingdom
[7]Present address: UK Dementia Research Institute, Imperial College, London, United Kingdom
[8]These authors contributed equally to this work as senior authors

Corresponding authors:
Anders Bach, Department of Drug Design and Pharmacology, Faculty of Health and Medical Sciences, University of Copenhagen, Universitetsparken 2, DK-2100 Copenhagen, Denmark. Email: anders.bach@sund.ku.dk.

Kate L. Lambertsen, Department of Neurobiology Research, Institute of Molecular Medicine, University of Southern Denmark, J.B. Winsloewsvej 21, DK-5000 Odense, Denmark. Email: klambertsen@health.sdu.dk.

Kristian Strømgaard, Department of Drug Design and Pharmacology, Faculty of Health and Medical Sciences, University of Copenhagen, Universitetsparken 2, DK-2100 Copenhagen, Denmark. Email: kristian.stromgaard@sund.ku.dk.

Abstract

Inhibition of postsynaptic density protein-95 (PSD-95) decouples *N*-methyl-D-aspartate (NMDA) receptor downstream signaling and results in neuroprotection after focal cerebral ischemia. We have previously developed UCCB01-144, a potent dimeric PSD-95 inhibitor, which binds PSD-95 with high affinity and is neuroprotective in experimental stroke. Here, we investigate the selectivity, efficacy and toxicity of UCCB01-144 and compare with the monomeric drug candidate Tat-NR2B9c. Fluorescence polarization using purified proteins and pull-downs of mouse brain lysates showed that UCCB01-144 potently binds all four PSD-95-like membrane-associated guanylate kinases (MAGUKs). In addition, UCCB01-144 affected NMDA receptor signaling pathways in ischemic brain tissue. UCCB01-144 reduced infarct size in young and aged male mice at various doses when administered 30 min after permanent middle cerebral artery occlusion, but UCCB01-144 was not effective in young male mice when administered 1 hour post-ischemia or in female mice. Furthermore, UCCB01-144 was neuroprotective in a transient stroke model in rats, and in contrast to Tat-NR2B9c, high dose of UCCB01-144 did not lead to significant changes in mean arterial blood pressure or heart rate. Overall, UCCB01-144 is a potent MAGUK inhibitor that reduces neurotoxic PSD-95-mediated signaling and improves neuronal survival following focal brain ischemia in rodents under various conditions and without causing cardiovascular side effects, which encourages further studies towards clinical stroke trials.

Selectivity, efficacy and toxicity studies of UCCB01-144, a dimeric neuroprotective PSD-95 inhibitor

Anders Bach[a, 1], Bettina H. Clausen[b, c, 1], Lotte K. Kristensen[d, 2], Maria G. Andersen[b, 3], Ditte Gry Ellman[b], Pernille B. L. Hansen[e, 4], Henrik Hasseldam[d], Marc Heitz[a, 5], Dennis Özcelik[a], Ellie J. Tuck[f, 6], Maksym V. Kopanitsa[f, 7], Seth G. N. Grant[g], Karin Lykke-Hartmann[h], Flemming F. Johansen[d], Kate L. Lambertsen[b, c, i, 8], Kristian Strømgaard[a, 8]

[a]Department of Drug Design and Pharmacology, University of Copenhagen, Copenhagen, Denmark.
[b]Department of Neurobiology Research, Institute of Molecular Medicine, University of Southern Denmark, Odense, Denmark.
[c]BRIDGE - Brain Research - Inter-Disciplinary Guided Excellence, Department of Clinical Research, University of Southern Denmark, Odense, Denmark.
[d]Molecular Pathology Section, BRIC, Copenhagen Biocenter, University of Copenhagen, Copenhagen, Denmark.
[e]Department of Cardiovascular and Renal Research, Institute of Molecular Medicine, University of Southern Denmark, Odense, Denmark.
[f]Synome Ltd, Babraham Research Campus, Cambridge, United Kingdom
[g]Centre for Clinical Brain Sciences, University of Edinburgh, Edinburgh, United Kingdom
[h]Department of Biomedicine and Department of Clinical Medicine, University of Aarhus, Aarhus, Denmark and and the Department of Clinical Genetics, Aarhus University Hospital, Aarhus, Denmark.
[i]Department of Neurology, Odense University Hospital, Odense, Denmark

[1]These authors contributed equally to this work as first authors
[2]Present address: Minerva Imaging, Copenhagen, Denmark; and Department of Clinical Physiology, Nuclear Medicine & PET and Cluster for Molecular Imaging, Department of Biomedical Sciences, Rigshospitalet and University of Copenhagen, Denmark
[3]Present address: ALK-Abelló A/S, Hørsholm, Denmark
[4]Present address: Cardiovascular, Renal and Metabolic, IMED Biotech Unit, AstraZeneca, Gothenburg, Sweden
[5]Present address: Department of Chemistry and Biochemistry, University of Bern, Bern, Switzerland
[6]Present address: The Gurdon Institute, University of Cambridge, Cambridge, United Kingdom
[7]Present address: UK Dementia Research Institute, Imperial College, London, United Kingdom
[8]These authors contributed equally to this work as senior authors

Corresponding authors:
Anders Bach, Department of Drug Design and Pharmacology, Faculty of Health and Medical Sciences, University of Copenhagen, Universitetsparken 2, DK-2100 Copenhagen, Denmark. Email: anders.bach@sund.ku.dk.

Kate L. Lambertsen, Department of Neurobiology Research, Institute of Molecular Medicine, University of Southern Denmark, J.B. Winsloewsvej 21, DK-5000 Odense, Denmark. Email: klambertsen@health.sdu.dk.

Kristian Strømgaard, Department of Drug Design and Pharmacology, Faculty of Health and Medical Sciences, University of Copenhagen, Universitetsparken 2, DK-2100 Copenhagen, Denmark. Email: kristian.stromgaard@sund.ku.dk.

Abstract

Inhibition of postsynaptic density protein-95 (PSD-95) decouples *N*-methyl-D-aspartate (NMDA) receptor downstream signaling and results in neuroprotection after focal cerebral ischemia. We have previously developed UCCB01-144, a potent dimeric PSD-95 inhibitor, which binds PSD-95 with high affinity and is neuroprotective in experimental stroke. Here, we investigate the selectivity, efficacy and toxicity of UCCB01-144 and compare with the monomeric drug candidate Tat-NR2B9c. Fluorescence polarization using purified proteins and pull-downs of mouse brain lysates showed that UCCB01-144 potently binds all four PSD-95-like membrane-associated guanylate kinases (MAGUKs). In addition, UCCB01-144 affected NMDA receptor signaling pathways in ischemic brain tissue. UCCB01-144 reduced infarct size in young and aged male mice at various doses when administered 30 min after permanent middle cerebral artery occlusion, but UCCB01-144 was not effective in young male mice when administered 1 hour post-ischemia or in female mice. Furthermore, UCCB01-144 was neuroprotective in a transient stroke model in rats, and in contrast to Tat-NR2B9c, high dose of UCCB01-144 did not lead to significant changes in mean arterial blood pressure or heart rate. Overall, UCCB01-144 is a potent MAGUK inhibitor that reduces neurotoxic PSD-95-mediated signaling and improves neuronal survival following focal brain ischemia in rodents under various conditions and without causing cardiovascular side effects, which encourages further studies towards clinical stroke trials.

Keywords: Dimeric inhibitor, ischemic stroke, MAGUKs, neuroprotection, PSD-95.

Abbreviations: CREB, cAMP response element-binding protein; FP, fluorescence polarization; HR, heart rate; MABP, mean arterial blood pressure; MAGUKs, membrane-associated guanylate kinases; NMDA, *N*-methyl-D-aspartate; nNOS, neuronal nitric oxide synthase; NO, nitric oxide; PDZ, PSD-95/Discs-large/ZO-1; p-ERK1/2, phosphorylated extracellular signal-regulated kinase 1/2; p-JNK1/2, phosphorylated c-Jun *N*-terminal protein kinase 1/2; pMCAO, permanent middle cerebral artery occlusion; PSD-95, postsynaptic density protein-95; tMCAO, transient middle cerebral artery occlusion; tPA, tissue plasminogen activator.

1. Introduction

PSD-95 is a scaffolding protein in neuronal synapses that interacts with *N*-methyl-D-aspartate (NMDA) receptors and neuronal nitric oxide synthase (nNOS) through its PSD-95/Discs-large/ZO-1 (PDZ) domains. When glutamate is released from presynaptic vesicles, it activates postsynaptic NMDA receptors leading to Ca^{2+} influx and nitric oxide (NO) production (Christopherson et al., 1999; Sattler et al., 1999). During cerebral ischemia, excessive glutamate release leads to hyperactivation of the NMDA receptors and harmful elevation of intracellular levels of Ca^{2+} and NO, which ultimately induces excitotoxicity, leading to neuronal death and brain damage (Aarts et al., 2002; Dawson et al., 1991; Huang et al., 1994; Sattler et al., 1999).

PSD-95 is currently being explored as a drug target in acute ischemic stroke and related ischemic conditions in the brain, and two peptide-based compounds seem particularly promising (Aarts et al., 2002; Bach et al., 2012). The 20-mer peptide Tat-NR2B9c (Fig. 1A) was designed by fusing the nine C-terminal amino acids of the GluN2B subunit to a HIV-1-derived Tat peptide to facilitate permeability across the blood-brain barrier and cell membranes (Aarts et al., 2002). Tat-NR2B9c binds to the PDZ1 and PDZ2 domains of PSD-95 and thereby blocks the formation of the nNOS/PSD-95/NMDA receptor complex and uncouples NMDA receptor activity from harmful NO production (Aarts et al., 2002). As Tat-NR2B9c does not affect the ion current through the NMDA receptor, it is believed that PSD-95 inhibition provides a more efficient and safe alternative compared to NMDA receptor antagonists as drug candidates of ischemic brain damage (Aarts et al., 2002; Soriano et al., 2008). Tat-NR2B9c has shown extensive neuroprotective effects in rats and non-human primate ischemic stroke models with a 1–3 h therapeutic time window (Aarts et al., 2002; Cook et al., 2012a, b). Furthermore, Tat-NR2B9c has been tested in a phase 2 clinical trial (under the name NA-1), where it met its primary safety endpoints and reduced the number of small infarcts in patients undergoing endovascular aneurysm repair (Hill et al., 2012). No effects were observed on total infarct volume or clinical outcome, perhaps due to limited group size (Hill et al., 2012), but future clinical studies are expected to elucidate the full potential of Tat-NR2B9c as a drug for stroke treatment (Ballarin and Tymianski, 2018).

Prompted by the relatively low affinity of Tat-NR2B9c, we designed the dimeric compounds Tat-*N*-dimer and *O*-dimer, also known as UCCB01-144 and UCCB01-125, respectively (Fig. 1A) (Bach et al., 2009; Bach et al., 2012; Kucharz et al., 2017). In an in vitro fluorescence polarization (FP) assay the K_i values of Tat-NR2B9c towards PDZ1 and PDZ2 of PSD-95 were 5–10 μM (Bach et al., 2008; Bach et al., 2012). In contrast, UCCB01-144 and UCCB01-125, due to their dimeric structures and bivalent properties, bind PDZ1 and PDZ2 of PSD-95 simultaneously, leading to a 500–1,000-fold higher affinity towards PDZ1–2 (K_i value of 4.6 and 9.5 nM, respectively) relative to that of monomeric Tat-NR2B9c (Bach et al., 2012). In mice that underwent permanent middle cerebral artery occlusion (pMCAO), a single intravenous (i.v.) bolus injection of UCCB01-144 (3 nmol/g) given 30 min post-ischemia reduced the infarct volumes by 40% and 37% at 6 h and 48 h of the post-ischemic survival period, respectively, compared to the effect of saline (Bach et al., 2012). Furthermore, functional outcomes such as grip strength and rotarod performance were improved and thus correlated with reductions in infarct size. Under the same experimental conditions and dose (3 nmol/g), Tat-NR2B9c did not show significant neuroprotective properties (Bach et al., 2012). Likewise, UCCB01-125 without the Tat moiety did not reach the brain and showed no neuroprotective properties (Bach et al., 2012).

In this study, we thoroughly investigated the neuroprotective properties of UCCB01-144 and compared it with the drug candidate Tat-NR2B9c. First, we examined the specificity of the compounds towards PSD-95 and homolog proteins from the membrane-associated guanylate kinase (MAGUK) protein family and investigated how UCCB01-144 affected signaling pathways downstream of PSD-95 in focal cerebral ischemia. We then tested the compounds in the mouse pMCAO model at various doses, time points, postnatal ages, and in both

sexes, as well as in the rat transient MCAO model (tMCAO). Finally, systemic blood pressure and heart rate were measured to address potential adverse cardiovascular effects related, in particular, to high compound doses.

2. Materials and Methods

2.1. In vitro studies

2.1.1. Fluorescence polarization (FP) assay

Affinities of the compounds (UCCB01-144, UCCB01-125, and Tat-NR2B9c) towards PDZ1–2 domains of the MAGUK proteins PSD-95 (Bach et al., 2012), PSD-93 (Fiorentini et al., 2013), SAP-97 (Chi et al., 2011), and SAP-102, respectively, were determined by FP as previously described for PSD-95 (Bach et al., 2012). Affinities towards PDZ2 and PDZ3 of PSD-95 were determined as previously described (Bach et al., 2008). Human SAP-102-PDZ1–2 was obtained in a pET151/D-TOPO expression vector from GeneArt Gene Synthesis (Thermo Fisher Scientific). Protein was expressed as His6-V5-TEV-SAP-102-PDZ1–2 in E. *coli* BL21(DE3)pLys strains (Invitrogen) at 25 °C for 16 h in LB media containing 100 µg/mL ampicillin and supplemented with 0.5 mM IPTG. Cells were harvested in phosphate buffer (50 mM NaPi, pH 7.4) with 10 mM $MgCl_2$, 1 mM PMSF, and cOmplete protease inhibitor tablets (Roche). Expressed protein was purified by Ni-affinity chromatography (HisTrap FF crude, GE Healthcare) and subsequent size-exclusion-chromatography (HiLoad 16/600 Superdex75, GE Healthcare) in HEPES buffer (25 mM HEPES, pH 7.4; 500 mM NaCl). Purified protein solution was supplemented with 1 mM EDTA and concentration was measured by UV spectroscopy using NanoDrop 1000 (Thermo Scientific). Correct mass was confirmed by ESI-LCMS (Agilent, Poroshell, 300SB-C18, 2.1 × 75 mm) and purity was determined via RP-UPLC (Waters Acquity).

2.1.2. Pull-down and western blotting of non-ischemic brain lysates

Biotin-labeled PSD-95 inhibitors were synthesized by solid-phase peptide synthesis, as previously described (Bach et al., 2012). Biotin was coupled to the *N*-terminal Fmoc deprotected amino group of the resin-bound intermediate, i.e. UCCB01-144-resin or Tat-NR2B9c-resin, to provide Biotin-UCCB01-144 and Biotin-Tat-NR2B9c, respectively. Likewise, Biotin-UCCB01-125 was obtained by coupling biotin to the secondary amine of resin-bound *N*-dimer (Bach et al., 2012).

Immunoprecipitation was performed using extracts from forebrains of 10–12-week-old C57BL/6J^{Babr} mice (Charles River Laboratories, Margate, UK). Tissue was homogenized in sodium deoxycholate buffer and incubated on ice for 1 h before spinning down at 20,000 rpm for 20 min, and the supernatant was collected. Biotin-labeled PSD-95 peptide inhibitors were bound to streptavidin-conjugated resin (Thermo Scientific, Loughborough, UK) by incubating 2.5 mM of each peptide with 120 µL of resin in Tris buffer containing 0.05% sodium deoxycholate. Resin and peptide solution were incubated for 3 h at room temperature before the peptide supernatant was removed and resin was washed with sodium deoxycholate buffer and stored at 4 °C. Peptide-coupled resin was aliquoted into 5×20 µL samples before adding protein lysate. The lysate was added at different protein-to-resin ratios: 1:10, 1:50, 1:100, 1:500, 1:1,000 and rotated at 4 °C overnight. Samples were spun down before flow-through samples were collected from each condition, and the remaining supernatant was discarded. Resin was thoroughly washed with sodium deoxycholate buffer before eluting the protein by heating to 70 °C for 30 min in elution buffer containing 1 × sample buffer and 10% β-mercaptoethanol. Using Pierce™ bicinchoninic acid assay (BCA) protein quantitation kit (Thermo Scientific, Loughborough, UK) input protein lysates were diluted to 2 µg/µL and each flow-through sample was diluted using the same ratio as for respective protein lysates. Samples were run on SDS-PAGE gels and blots were

probed for MAGUK proteins using primary antibodies against PSD-95 (cat. No. MA1-045, Thermo Scientific, Loughborough, UK), PSD-93 (cat. No. 75-057; NeuroMab, Davis, CA), SAP97 (cat. No. 75-030; NeuroMab, Davis, CA), and SAP102 (cat. No. 124202; Synaptic Systems, Göttingen, Germany). Primary antibodies were incubated overnight before washing and applying horseradish peroxidase (HRP) secondary antibodies for 1 h at room temperature. Blots were visualized using Pierce™ ECL Western Blotting Substrate (Thermo Scientific, Loughborough, UK) on a GE Healthcare Life Sciences ImageQuant 4000 imager. As negative control for primary antibodies, we used protein lysates from hippocampal tissue of previously described mutant mice bearing loss-of-function mutations in *Dlg1*, *Dlg2*, *Dlg3* and *Dlg4* genes, encoding SAP-97, PSD-93, SAP102 and PSD-95 proteins, correspondingly (Carlisle et al., 2008; Cuthbert et al., 2007; Migaud et al., 1998).

2.1.3. Western blotting for nNOS and phosphorylated ERK1/2 and JNK1/2

Western blotting analyses for phospho-ERK1/2, phospho-JNK1/2, and nNOS were performed as described previously (Clausen et al., 2016) using 40 μg of protein extract. Whole-brain tissue homogenates from mice that underwent pMCAO or sham surgery and were treated with 3 nmol/g UCCB01-144 or 3 nmol/g Tat-NR2B9c and survived for 6 or 48 h originated from a previous study (Bach et al., 2012). Groups consisted of sham animals (n = 3/time point), saline-treated mice (n = 6/time point), UCCB01-144-treated mice (n = 6/time point), and Tat-NR2B9c-treated mice (n = 6/time point). Proteins were separated on 10% SDS-PAGE gels, with all groups represented randomly across the three gels, and visualized using anti-nNOS (1:1,000; Cell Signaling Technology), anti-phospho-ERK1/2 (1:1,000; Cell Signaling Technology), and anti-phospho-JNK1/2 (1:1,000; Cell Signaling Technology) antibodies. Glyceraldehyde-3-phosphate dehydrogenase (GAPDH) was measured with an anti-GAPDH antibody (Cell Signaling Technology) as loading control. Proteins were quantified by densitometry using ImageJ (NIH, USA). The relative intensities of the bands were compared to the background (gray scale), and data from all the samples were normalized by the intensity of loading control signal (GAPDH).

2.1.4. ELISA procedure for measuring estradiol levels in serum

Blood (approximately 200–300 μL) from individual mice was collected from the neck after decapitation and allowed to clot for 30 min at room temperature. The samples were centrifuged at ~2,000×g at 4 °C for 15 min. The serum was transferred to new tubes, and the centrifugation step was repeated. Serum was aliquoted and stored at −80 °C. The estradiol assay protocol (Mouse/Rat Estradiol ELISA ES180S-100, Calbiotech Inc, Spring Valley, CA, USA) was followed, and 2×25 μL serum was analyzed for the estradiol level (pg/mL) according to the manufacturer´s instructions (Bottger et al., 2016).

2.2. pMCAO in mice

2.2.1 Animals and ethical statement

The study was performed using age-matched, young adult (7–8 weeks) male and female C57BL/6J mice (Taconic) as well as aged (12 months) male C57BL/6J mice (Charles River). Mice were housed in separate cages under diurnal lighting and given free access to food (1314 Altromin) and water. Mice were allowed to acclimatize for one week prior to the experiments and cared for in accordance with the protocols and guidelines approved by The Danish Animal Inspectorate under the Ministry of Food and Agriculture (J. number 2013-15-2934-00924). The experiments are reported in accordance with the ARRIVE (Animal Research: Reporting of In Vivo Experiments) guidelines, and all efforts had been made to minimize pain and distress.

2.2.2. Surgical procedure and infarct volumetry

Mice were subjected to pMCAO as previously described (Bach et al., 2012) under Hypnorm™ (fentanyl citrate 0.315 mg⁄mL and fluanisone 10 mg⁄mL, VectaPharma Ltd) and midazolam (5 mg⁄mL, Hameln) anesthesia. Brain tissue was processed as previously described in detail (Bach et al., 2012). Infarct volumetric analysis was performed on toluidine blue-stained tissue sections as previously described in detail (Lambertsen et al., 2001). For management of postsurgical pain, animals were supplied with Temgesic (0.001 mg⁄20 g buprenorphinum, Reckitt & Coleman) three times with an 8 h interval, starting immediately prior to surgery. In addition, the mice were injected subcutaneously with 1 mL of isotonic saline before being transferred to the controlled recovery room with ambient temperature 25 °C.

2.2.3. Drug administration and groups

Compounds were dissolved in isotonic (0.9%) saline (NaCl), randomized and blinded to the operator, and administered intravenously as a bolus into the tail vein using the following dosing protocols: *i*) 1 nmol/g UCCB01-144 (n = 20) into young adult, male C57BL/6J mice, 30 min after surgery; *ii*) 9 nmol/g UCCB01-144 (n = 20) or Tat-NR2B9c (n = 20) into young adult, male C57BL/6J mice, 30 min after surgery; *iii)* 30 nmol/g UCCB01-144 (n = 20) or Tat-NR2B9c (n = 30) into young adult, male C57BL/6J mice, 30 min after surgery; *iv*) 3 nmol/g UCCB01-144 (n = 15) into young adult, male C57BL/6 mice, 1 h after surgery; *v*) 9 nmol/g UCCB01-144 (n = 20) into aged, male C57BL/6 mice, 30 min after surgery; *vi*) 9 nmol/g UCCB01-144 (n = 27) into young adult, female C57BL/6 mice, 30 min after surgery; and *vii*) 9 nmol/g UCCB01-144 (n = 20) into young adult, Depo-provera-treated female C57BL/6 mice, 30 min after surgery. Separate groups of age-matched control mice (n = 15–28 mice/experiment) were included in each experiment and received an i.v. injection of 0.9% NaCl. Depo-provera® (50 mg/mL, Pfizer) diluted ×2.5 in isotonic saline (pH 7.4) was administered subcutaneously (2 mg Depo-provera/mouse) 3 weeks prior to pMCAO (Bottger et al., 2016). In total, 335 mice were used in these pMCAO studies.

Young adult female mice with or without Deproprovera pretreatment and aged male mice were treated with saline or 9 nmol/g UCCB01-144 i.v. 30 min after pMCAO and allowed 24 h survival. Of the 135 mice included, 22 mice were found not to have an infarct and were therefore excluded. In another experiment, young adult male mice treated with saline, 1, 9, or 30 nmol/g UCCB01-144, or 9 or 30 nmol/g Tat-NR2B9c i.v. 30 min after pMCAO were allowed 48 h survival, as were mice treated with 3 nmol/g UCCB01-144 60 min after pMCAO. Of the 200 mice included here, two mice died during anesthesia, and 28 mice treated with 30 nmol/g Tat-NR2B9c died immediately after drug injection. In addition, 34 mice were found not to have an infarct and were therefore excluded.

2.3. tMCAO in rats

2.3.1. Animals and ethical statement

This study was approved and conducted according to the protocols and guidelines approved by The Danish Animal Inspectorate under the Ministry of Food and Agriculture (J. No. 2013-15-2934-00950). All procedures, including steps to eliminate animal suffering, were carried out and reported in accordance with ARRIVE guidelines. In total, 45 adult male Sprague-Dawley rats (10–12 weeks old, 275–300 g) were included in the study. Of these, 15 rats were excluded; among them seven rats died during the surgery because the filament penetrated the artery and caused a severe subarachnoid hemorrhage, whereas the remaining eight rats were terminated because of other technical problems. The remaining 30 animals were included in the study and distributed among treatment groups as indicated in section 2.3.3.

2.3.2. Surgical procedure and infarct volumetry

All experiments were performed on animals that fasted for 12 h with free access to water during that period. At 15 min before surgery, the animals were anesthetized by i.p. administration of 2.7 mL/kg body weight hypnorm/midazolam (2.5 mg/mL fluanisone and 0.079 mg/mL fentanyl citrate, 1.25 mg/mL midazolam, ScanVet, Denmark). In order to maintain anesthesia, the animals received half of this dose 30–40 min later. The femoral artery was canalized and pCO_2, pO_2, blood gasses, electrolytes, and blood glucose (Radiometer ABL700; Radiometer Medical, Copenhagen, Denmark) were monitored before, during, and immediately after surgery. The right middle cerebral artery was occluded by the intraluminal suture method of Longa et al. (Longa et al., 1989). Briefly, a nylon monofilament (#37, Doccol, Sharon, MA, USA) was inserted through the right carotid artery and advanced intracranially to block blood flow to the middle cerebral artery. After 90 min, the filament was gently removed backwards, and the animals had 23 h of reperfusion before they were euthanized. A successful occlusion of the middle cerebral artery resulted in complete dilation of the pupil in the ipsilateral side, immediately after the filament was in place. Reperfusion, on the contrary, resulted in a prompt hyperemic flush with distinct red color of the ischemic pale eye. Body core temperature was maintained at 37.0 ± 0.1 °C during surgery, using a heat lamp.

Animals received a lethal i.p. injection with 150 mg/kg sodium pentobarbital and 50 mg/mL lidocaine (1% lidocaine)(ScanVet) 24 h after surgery, followed by the perfusion with 50 mL saline and 150 mL formalin (Hounisen, Denmark). The brains were removed, immersion-post-fixed in 10% formalin (Hounisen) for 24 h at 4 °C, dehydrated, and embedded in paraffin according to standard procedures. Coronal sections (3 µm) were cut at 400 µm intervals, mounted, and stained with hematoxylin and eosin (H&E, Sigma-Aldrich). The H&E-stained sections were scanned by using NanoZoomer-XR (Hamamatzu, Japan) and infarct size was quantified with NDP.View2 software viewer (Hamamatsu Photonics) according to the principles of Bonaventura Francesco Cavalieri adjusted to modern guidelines (Bonfils et al., 2006). Briefly, the area of the surviving tissue in the infarcted hemisphere was subtracted from the area of the contralateral non-infarcted hemisphere in order to obtain the area of the infarct. This was then multiplied by the distance between the levels (400 µm), in order to obtain the infarct volume.

2.3.3. Drug administration and groups

Rats were treated with 1 mL/kg of saline (n = 9), UCCB01-144 (3 nmol/g, n = 11) or Tat-NR2B9c (3 nmol/g, n = 10) through the tail vein 30 min before reperfusion. The drugs were chosen in a random fashion and blinded to the operator prior to administration.

2.4. Cardiovascular studies

The experimental protocol was approved by the Danish Animal Experiments Inspectorate under the Danish Ministry of Justice (2015-15-0201-00479) and animal care followed the guidelines of the National Institutes of Health in accordance with ARRIVE guidelines. The experimental procedures have been described previously (Andersen et al., 2011; Hansen et al., 2010; Laursen et al., 2018). Mice were anesthetized (100 mg/kg ketamine, 10 mg/kg xylazine) and chronic indwelling catheters were surgically implanted in the femoral artery for measurements of mean arterial blood pressure (MABP) and heart rate (HR), and into the femoral vein for drug infusions. Arterial and venous catheters consisted of a micro-renathane tip (0.34–0.38 mm outer diameter) connected to a polyethylene tubing. The catheters were tunneled subcutaneously and led externally through a 15 cm spring. The spring was attached to the back of the animal by sewing a 1 cm stainless steel button into the strap muscles between the scapulae. Following the operation, the catheters were attached to a

swivel enabling the mice to move freely and each mouse was caged separately. To maintain catheter opening, a heparin solution (100 IU/mL in isotonic glucose) was infused at the arterial side at 10 µL/h. After 5 days, the mice had fully recovered and continuous measurements of MABP and HR were initiated. Arterial pressure was measured by connecting the arterial line to solid-state pressure transducers (Föhr Medical Instruments, Hessen, Germany) and using a general-purpose amplifier. Amplified signals were fed into an analog-to-digital converter and the data were collected at 200 Hz to obtain periodic (15–300 s) averages of systolic pressure, diastolic pressure, MABP, and HR using Lab View software (National Instruments, Austin, TX, USA).

On day 5, basal blood pressure and HR were measured for 2 h followed by 50 µL bolus infusions of either PSD-95 inhibitors or saline through the venous catheter. Initially, an isotonic glucose/heparin bolus was given to ensure the correct placement of drug or vehicle in the dead space of the catheter. In total, 17 C57Bl/6J male and female mice (Taconic, Denmark) were randomly assigned to three different groups that were treated with either vehicle (saline) (n = 4), UCCB01-144 (n = 8), or Tat-NR2B9c (n = 6). Three different doses of each compound were tested over a period of 4 h. MABP and HR were monitored for 2 h after either a 3 or 9 nmol/g dose followed by 2 h of monitoring after either a 9 nmol/g or 30 nmol/g dose.

3. Results

3.1. Selectivity of binding to different MAGUKs

The PSD-95 family of MAGUK proteins comprises PSD-95, PSD-93, SAP-97, and SAP-102. These proteins share a highly similar overall architecture comprising three PDZ domains, one Src-homology 3 domain, and one catalytically inactive guanylate kinase domain. These proteins are all found in neuronal synapses, where they serve as scaffolding proteins involved in anchoring and trafficking of glutamate receptors as well as of other membrane proteins (Feng and Zhang, 2009; Frank et al., 2016). Due to their high sequence homology and functional overlap, we investigated the in vitro selectivity of UCCB01-144 and Tat-NR2B9c binding to the four MAGUK proteins. UCCB01-144, UCCB01-125, and Tat-NR2B9c were tested against PDZ1–2 of PSD-93, SAP-97 and SAP-102 in an in vitro FP assay identical to the assay that showed a K_i of 4.6 nM for binding between UCCB01-144 and PSD-95-PDZ1–2 (Bach et al., 2012). Generally, we found no significant differences in the parameters of binding of peptide-based inhibitors to the four PDZ1–2 domains. PDZ1–2 of all four MAGUK proteins bound UCCB01-144 and UCCB01-125 with low nanomolar affinity (K_i = 1–7 nM and 6–22 nM, respectively) and Tat-NR2B9c with K_i values in the micromolar range (K_i = 2–5 µM) (Fig. 1B, Table 1). When tested towards individual PDZ domains from PSD-95, UCCB01-144 and UCCB01-125 bound to them with K_i values of 1 µM for PDZ2 and 50–87 µM for PDZ3 (Fig. 1B, Table 1). Tat-NR2B9c binds PSD-95-PDZ2 with the same affinity (K_i = 4.4 µM) as to PSD-95-PDZ1–2, but it does not bind PDZ3 (Table 1) (Bach et al., 2008). Thus, the PSD-95 inhibitors tested here – dimeric (UCCB01-144, UCCB01-125) and monomeric (Tat-NR2B9c) – did not show selective in vitro binding to PSD-95 over that to the other MAGUK proteins PSD-93, SAP-97, and SAP-102. These data also confirm much (100–1,600 fold) stronger binding affinity of dimeric inhibitors to MAGUK PDZ1–2 domains in comparison to that of monomeric Tat-NR2B9c. This increased affinity can be explained by the bivalent binding mode of UCCB01-125/144, as two ligand moieties bind PDZ1 and PDZ2 simultaneously (Bach et al., 2012).

We next explored if the compounds bound to MAGUK proteins of the PSD-95 family in a more complex biological environment. Thus, we added biotin-labeled analogs of the compounds to a homogenous lysate of adult mouse forebrain, pulled down the compounds (and interacting proteins) using streptavidin resin, and analyzed the precipitate by SDS-PAGE and western blotting with antibodies for the four homologous MAGUK proteins: PSD-95, PSD-93, SAP-97, and SAP-102. We found that UCCB01-144, UCCB01-125, and Tat-NR2B9c

pulled down all four MAGUK proteins (Fig. 1C). UCCB01-144 was most efficient in pulling down PSD-95, and UCCB01-125 was least efficient. Control compounds, i.e. analogs of UCCB01-144, UCCB01-125, and Tat-NR2B9c without the essential C-terminal valine residue, which cannot bind to PSD-95, did not pull down any of the MAGUK proteins (data not shown).

3.2. Signaling pathways affected by UCCB01-144 in the brain of ischemic mice

Having demonstrated that UCCB01-144 binds to PSD-95 and related MAGUKs in the relevant biological environment (mouse brain tissue lysate), we next explored if the compound affected PSD-95-related signaling pathways in animals with focal cerebral ischemia. Previous studies using fluorescently labeled versions of UCCB01-144 have demonstrated its brain permeability in non-ischemic animals (Bach et al., 2012; Kucharz et al., 2017). Furthermore, staining of UCCB01-144 with an anti-Tat antibody in brain slices from mice subjected to focal cerebral ischemia and treated with the compound indicated the presence of UCCB01-144 in neurons (Bach et al., 2012). Here, by using western blotting with antibodies against nNOS, phosphorylated c-Jun *N*-terminal protein kinase 1/2 (p-JNK1/2), and extracellular signal-regulated kinase 1/2 (p-ERK1/2), we analyzed whole-brain tissue from pMCAO mice, in which UCCB01-144 reduced infarct size by 40% (6 h survival study) or 37% (48 h survival study) of control values (Bach et al., 2012).

Both Tat-NR2B9c and UCCB01-144 reduced nNOS expression relative to saline-treatment at 6 h after pMCAO with an overall effect identified by one-way ANOVA ($F(3, 17) = 8.30$, $p = 0.0013$) and Dunnett's multiple comparisons test between treatment groups ($p = 0.0022$, saline vs Tat-NR2B9c; $p = 0.0011$, saline vs UCCB01-144) (Fig. 2A). At 48 h, a similar pattern was seen, but the effect was not statistically significant ($F(3, 17) = 1.05$, $p = 0.40$) (Fig. 2B). Two p-JNK bands were seen on western blots that corresponded to the two p-JNK1/2-isoforms (46 and 54 kDa). At 6 h, an almost 10-fold increase in p-JNK1/2 was seen in the ischemia groups (saline, UCCB01-144, Tat-NR2B9c) relative to the level in sham mice ($F(3, 17) = 11.8$, $p = 0.0002$, one-way ANOVA), but none of the compounds reduced p-JNK1/2 from the level observed in saline-treated ischemic animals (Fig. 2C). At 48 h, p-JNK1/2 levels were back to the levels seen in sham mice (Fig. 2D). The level of p-ERK1/2 isoforms was found to be increased in UCCB01-144-treated animals compared to those in saline-treated mice (one-way ANOVA: $F(3, 17) = 7.14$, $p = 0.0026$. Dunnett's multiple comparisons of treatment groups: $p = 0.0011$, saline vs UCCB01-144) at 6 h (Fig. 2E), but not at 48 h (Fig. 2F).

3.3. Effect in the pMCAO model in mice

We explored the dose-response relationship of dimeric UCCB01-144 and monomeric Tat-NR2B9c in the pMCAO mouse model of focal ischemia. Previously, we tested both compounds at 3 nmol/g (i.v. bolus injection 30 min post-ischemia) in this model, and whereas UCCB01-144 reduced the infarct size by 37% (48 h survival), no statistically significant infarct reduction by Tat-NR2B9c was observed (Bach et al., 2012). Here, in three independent experiments (Fig. 3A–C, respectively), we tested UCCB01-144 at 1, 9, and 30 nmol/g and Tat-NR2B9c at 9 and 30 nmol/g. As in the previous study, i.v. injection was given 30 min post-ischemia and the survival period was 48 h. UCCB01-144 did not reduce infarct volume at 1 or 30 nmol/g relative to the infarct volume level in saline-treated young male mice ($t(31) = 0.557$, $p = 0.58$, 1 nmol/g dose; $t(30) = 0.558$, $p = 0.58$, 30 nmol/g dose; Student's two-tailed unpaired t-test; Fig. 3A and C, respectively), but at 9 nmol/g, a 37% infarct reduction was seen (one-way ANOVA: $F(2, 45) = 5.00$, $p = 0.011$; followed by the Tukey's multiple comparisons test: $p = 0.011$, saline vs UCCB01-144; Fig. 3B). Tat-NR2B9c at 9 nmol/g reduced infarct volume by 32% relative to saline-treated mice (Tukey's multiple comparisons test: $p = 0.036$, saline vs Tat-NR2B9c; Fig. 3B), thereby confirming the neuroprotective effect demonstrated in literature of this monomeric PSD-95

inhibitor. However, when Tat-NR2B9c was administered to mice at 30 nmol/g, 28 out of 30 mice died immediately after drug injection indicating acute toxicity of Tat-NR2B9c at this high dose.

Next, we explored the therapeutic time window of UCCB01-144 in the pMCAO model. UCCB01-144 was injected 60 min post-ischemia (i.v., 3 nmol/g, 48 h survival), and although a trend towards infarct reduction was seen, the difference between infarct size in saline- and UCCB01-144-treated groups did not reach statistical significance ($t(21) = 1.29$, $p = 0.21$; Student's two-tailed, unpaired t-test; Fig. 3D).

Biological variation is a critical parameter to investigate for any potential stroke candidate. We therefore explored neuroprotective properties of UCCB01-144 in aged (12 months) male mice and in young female mice injected with 9 nmol/g UCCB01-144 (30 min post-ischemia) and sacrificed after a 24 h survival period. A 28% infarct reduction was seen in aged male mice ($t(33) = 2.59$, $p = 0.014$; Student's two-tailed, unpaired t-test; Fig. 3E), whereas no effect was observed in young female mice ($t(41) = 0.210$, $p = 0.83$; Student's two-tailed, unpaired t-test; Fig. 3F). We repeated the experiment in females after stabilizing and lowering their estradiol-levels (Supplementary Fig. 1) by using Depo-provera, a progestin-only contraceptive that suppresses the natural cyclic fluctuations of female sex hormones (Jeppsson et al., 1982). Nonetheless, we did not observe a statistical significant infarct reduction by UCCB01-144 ($t(33) = 0.209$, $p = 0.84$; Student's two-tailed, unpaired t-test; Fig. 3G).

3.4. Effect in the tMCAO model in rats

We evaluated neuroprotective effects of 3 nmol/g UCCB01-144 and Tat-NR2B9c in a rat model of transient ischemia (tMCAO model). The compounds were injected i.v. 60 min after occlusion (i.e., 30 min before reperfusion), and the rats were allowed a 24 h survival period. This dose, model, and timing were similar to those employed in the original study that showed neuroprotective effects of Tat-NR2B9c in vivo (Aarts et al., 2002). However, we did not find a statistical significant effect of Tat-NR2B9c on infarct volumes (one-way ANOVA: $F(2, 27) = 3.61$, $p = 0.0407$; followed by the Tukey's multiple comparisons test: $p = 0.47$, saline vs Tat-NR2B9c; Fig. 4A), although a trend towards reduced injury was observed ($t(17) = 1.32$, $p = 0.21$; Student's two-tailed, unpaired t-test, saline vs Tat-NR2B9c). Treatment with UCCB01-144, on the other hand, was associated with a 31% reduction in total infarct volume relative to saline-treated rats, with the effect evenly distributed across the brain sections ($p = 0.033$; one-way ANOVA followed by Tukey's multiple comparisons test; Fig. 4B).

3.5. Cardiovascular studies

Because UCCB01-144 at a high dose of 30 nmol/g did not affect infarct size, and Tat-NR2B9c at the same dose was toxic, killing almost all pMCAO-lesioned mice, we sought to explore whether those findings were related to cardiovascular side effects. It should be noted in this regard that a patent reports that Tat-NR2B9c induced profound lowering effect on blood pressure at higher doses in rats, Beagle dogs, and humans, thereby defining and limiting the maximum tolerated dose in humans to 2.6 mg/kg (~1 nmol/g) (Hill et al., 2012; Tymianski et al., 2011). This effect of Tat-NR2B9c on blood pressure came with increased levels of blood histamine and related side effects in dogs and humans and could be attenuated by a pre-treatment with the antihistamine benadryl in dogs (Tymianski et al., 2011). Additionally, SAP-97 is expressed in cardiomyocytes, where it associates with voltage-gated potassium channels, likely regulating their function (Milstein et al., 2012; Vaidyanathan et al., 2010). Thus, potentially, a SAP-97 or MAGUK inhibitor such as UCCB01-144 or Tat-NRB9c could affect cardiac excitability and rhythm. Those findings prompted us to explore if UCCB01-144 and Tat-NR2B9c affected the cardiovascular system.

MABP and HR were assessed in wild-type, non-ischemic mice, similar to those used in the pMCAO experiments, by continuous sampling every 5 min for 2 h before and 2 h after treatment with 3, 9, or 30 nmol/g UCCB01-144 or Tat-NR2B9c. No statistically significant MABP differences were observed between saline-treated mice and animals administered with 3 or 9 nmol/g UCCB01-144 (Fig. 5A) ($F(1, 7) = 2.63$, $p = 0.15$ (3 nmol/g); $F(1, 8) = 0.972$, $p = 0.35$ (9 nmol/g); two-way ANOVA followed by the Bonferroni's post-test for multiple comparisons to saline control at individual time points). An overall borderline significant difference in MABP across the experimental period was suggested by two-way ANOVA for mice given 30 nmol/g UCCB01-144 compared to saline ($F(1, 7) = 5.95$, $p = 0.045$), but the Bonferroni's post-test revealed no significant differences at individual time points (Fig. 5A). Similarly, treatment with Tat-NR2B9c did not result in any measurable changes in MABP ($F(1, 5) = 0.00272$, $p = 0.96$ (3 nmol/g); $F(1, 5) = 0.0781$, $p = 0.79$ (9 nmol/g); $F(1, 5) = 0.973$, $p = 0.37$ (30 nmol/g); two-way ANOVA followed by the Bonferroni's post-test) (Fig. 5B). At 3 and 9 nmol/g, no effects on HR were observed for UCCB01-144 relative to those in the saline-treated group ($F(1, 7) = 0.0680$, $p = 0.80$ (3 nmol/g); $F(1, 8) = 1.60$, $p = 0.24$ (9 nmol/g); two-way ANOVA followed by the Bonferroni's post-test), but at 30 nmol/g, a small but significant increase in HR compared to that in saline-treated mice was observed at 205–230 min ($F(1, 7) = 5.15$, $p = 0.057$ (30 nmol/g); two-way ANOVA. Bonferroni's post-test reveal significant differences with $p = 0.0019$–0.048 at individual time points as indicated at Fig. 5C). There was no effect of Tat-NR2B9c compared to that of saline on HR at 3 or 9 nmol/g ($F(1, 5) = 0.292$, $p = 0.61$ (3 nmol/g); $F(1, 5) = 0.601$, $p = 0.47$ (9 nmol/g)), but at 30 nmol/g, a dramatic drop was observed immediately after drug injection ($F(1, 5) = 0.149$, $p = 0.72$; two-way ANOVA. Bonferroni's post-test reveal significant differences with $p = 0.0048$–0.013 at 125–140 minutes as indicated at Fig. 5D), and HR did not return to normal level until after additional 20–30 min (Fig. 5D).

4. Discussion

We found that UCCB01-144 binds PSD-95 and other members of the MAGUK family through their PDZ1–2 domains with K_i values of 1–7 nM. These data emphasize that dimeric UCCB01-144 has a 300–1,600-fold higher affinity for MAGUKs than Tat-NR2B9c, a monomeric PSD-95 ligand with K_i of 2–5 μM. Accordingly, UCCB01-144 was more efficient in pulling down PSD-95 and the three closely related MAGUKs – PSD-93, SAP-97, and SAP-102 – from mouse brain lysates. This finding was in agreement with studies that showed no or little selectivity toward different MAGUK PDZ domains across a wide variety of peptide ligands (Lim et al., 2002; Stiffler et al., 2007), and with the finding that Tat-NR2B9c inhibited interactions with NMDA receptor-derived peptide ligands and PDZ2 from PSD-95, SAP-97, and PSD-93 in an ELISA-based assay (Cui et al., 2007). However, whereas suppressing PSD-95 expression using posttranscriptional silencing of the *Dlg4* gene protected primary cultured cortical neurons against NMDA-induced neurotoxicity, a similar effect was not observed when expression of other MAGUKs (SAP-97, PSD-93, and SAP-102) was downregulated, which points to PSD-95 as the most likely target of interest in relation to excitoxicity (Cui et al., 2007).

PSD-95 inhibitors such as UCCB01-144 and Tat-NR2B9c are assumed to block the association of nNOS and NMDA receptors with PSD-95 (Aarts et al., 2002; Bach et al., 2012; Zhou et al., 2010). Interestingly, western blotting of ischemic brain tissue revealed that both compounds reduced nNOS expression 6 h after pMCAO, an effect that would reinforce their neuroprotective properties in addition to the displacement of nNOS from the NMDA receptor complex. The pro-death signaling protein p-JNK1/2 was markedly increased in saline-treated ischemic mice relative to its level in non-ischemic mice, as was also shown by others in necrotic areas after focal brain ischemia (Wu et al., 2000), but UCCB01-144 and Tat-NR2B9c did not affect these enhanced p-

JNK1/2 levels. This observation was in line with the proposed mechanism of action of Tat-NR2B9c, which was shown to decrease the activity of p38-related pro-death pathways in neurons by lowering NO production, but without an effect on JNK-mediated pro-death signaling. Instead, JNK activation was initiated by mitochondrial production of reactive oxygen species (Soriano et al., 2008). In the same study (Soriano et al., 2008), it was shown that activation of pro-survival pathways in neurons, e.g., via cAMP response element-binding protein (CREB), were not affected by Tat-NR2B9c treatment. Here, we observed that the amount of p-ERK, which is upstream to pro-survival CREB (Hardingham, 2006; Hu et al., 2000; Lai et al., 2014), was higher in UCCB01-144-treated animals compared to that in saline- and Tat-NR2B9c-treated groups. Likewise, other studies of cerebral ischemia report that p-ERK upregulation correlates with the efficacy of various neuroprotectants (Sawe et al., 2008), such as a bisperoxovanadium phosphatase and tensin homolog (PTEN) inhibitor (Liu et al., 2018), leptin (Zhang and Chen, 2008), and combination treatment with progesterone and vitamin D (Atif et al., 2013). By pharmacological inhibition of ERK1/2, the neuroprotective effects of the PTEN inhibitor and leptin was shown to be mediated by ERK1/2. Whether p-ERK upregulation represents a difference in the mechanism of action of dimeric UCCB01-144, which binds to both PDZ1 and PDZ2 of PSD-95 simultaneously, and monomeric Tat-NR2B9c, which binds to only one of the PDZ domains at a time (Bach et al., 2012), or if the neuroprotective effect of UCCB01-144 depends on ERK1/2 activation should be elucidated by further studies exploring the two compounds across various stroke models and doses.

Overall, these data show that the PSD-95 inhibitor UCCB01-144 affects downstream signaling proteins in the NMDA receptor-triggered excitotoxic cascade in a way that correlates with the observed neuroprotective effects in vivo. Additional studies focusing on neurons or necrotic tissue could further elucidate the putative mechanism of action of UCCB01-144.

In this study, i.v. administration of UCCB01-144 and Tat-NR2B9c at 9 nmol/g reduced infarct volume in the pMCAO mouse model by 37% and 32%, respectively. For UCCB01-144, this confirms the previously published neuroprotective effect (37% infarct reduction) at the lower 3 nmol/g dose, where a correlation between infarct reduction and improved functional outcome was also observed (Bach et al., 2012). As the highest 30 nmol/g dose was not effective, this study also seems to establish that the maximum effect of UCCB01-144 is within 37–40% infarct size reduction in this model. For Tat-NR2B9c, the 32% infarct reduction at 9 nmol/g confirms the well-documented neuroprotective properties of this compound (Aarts et al., 2002; Bell et al., 2013; Bratane et al., 2011; Cook et al., 2012a, b; Hill et al., 2012; Soriano et al., 2008; Sun et al., 2008; Teves et al., 2016). Given the previously reported lack of effect of 3 nmol/g Tat-NR2B9c (Bach et al., 2012) and high toxicity at 30 nmol/g, this indicates that the effective therapeutic window is narrower for Tat-NR2B9c (effective at 9 nmol/g, but not at 3 or 30 nmol/g) than for UCCB01-144 (effective at 3 and 9 nmol/g, but not at 1 or 30 nmol/g) in our pMCAO mouse model. This outcome correlates with literature data on the efficacy of Tat-NR2B9c in a tMCAO mouse model, where a 3 nmol/g dose was ineffective, but 10 nmol/g reduced infarct size by 24–26% (Teves et al., 2016). Likewise, another study did not demonstrate any effects of 3 nmol/g Tat-NR2B9c on infarct size in their tMCAO mouse model, but that study also failed to show any effects of UCCB01-144 at the same dose (Kleinschnitz et al., 2016). It should be noted that our dose-response study is not conducted as a single experiment, but as four rounds of tests (Bach et al., 2012 and Fig. 3A-C), which could cause potential variations.

The fact that 30 nmol/g UCCB01-144 was not neuroprotective and the same dose of Tat-NR2B9c was lethal to pMCAO mice led us to investigate potential cardiovascular effects of the compounds in non-ischemic mice. This was further prompted by the fact that Tat-NR2B9c administration caused histamine release in dogs and

humans, leading to severe hypotension, reddening, swelling, and related symptoms. These side effects limited the dose used in clinical trials to 2.6 mg/kg (~1 nmol/g) (Hill et al., 2012; Tymianski et al., 2011), the same dose used in primate studies (Cook et al., 2012a, b). Further, SAP-97, which we here show is also targeted by both Tat-NR2B9c and UCCB01-144, is present in cardiac muscle cells. For UCCB01-144, we did not observe any clear effects on HR or MABP, so it is unlikely that the lack of neuroprotective effect at 30 nmol/g was due to detrimental modulation of cardiovascular functions. In the case of 30 nmol/g Tat-NR2B9c, however, there was a dramatic drop in HR immediately after administration, which did not normalize until after 20–30 min. These significant effects on HR indicate cardiovascular issues for Tat-NR2B9c, which could be related to the reported histamine-releasing properties, and seem less likely to be related to target-mediated effects via PSD-95 or off-target effects via SAP-97 as the HR drop was not seen for UCCB01-144. Also, these side effects likely also explain why the majority of ischemic mice, which are more vulnerable than non-ischemic mice, died in our hands after being given 30 nmol/g Tat-NR2B9c.

In our rat tMCAO study of Tat-NR2B9c and UCCB01-144, UCCB01-144 treatment was associated with a 31% reduction in total infarct volume relative to that in saline-treated rats. No statistically significant effect was seen for Tat-NR2B9c although a positive trend was observed, indicating that a higher dose might result in a significant effect. These findings do not correlate well with previous reports (reviewed in (Haugaard-Kedström et al., 2017)), where reductions in infarct size in rat tMCAO models were as high as 53–75% at Tat-NR2B9c doses as low as 0.03 nmol/g (Aarts et al., 2002; Sun et al., 2008). This discrepancy could be due to biological and surgical variations related to animal stroke models (Carmichael, 2005), or compound formulation. Here, Tat-NR2B9c was injected in a standard saline solution, like UCCB01-144.

The therapeutic time window of UCCB01-144 in the mouse pMCAO model is so far determined to be somewhere between 30 and 60 min post-stroke, as we observed no statistically significant effect on infarct volume when 3 nmol/g UCCB01-144 was administered 1 h post-ischemia. However, we have not investigated if a higher dose or altered dosing schemes, such as multiple injections or infusions, could extend this time window. Currently it is not known what the 30–60 minute therapeutic time-window in the pMCAO mouse model corresponds to in ischemic stroke patients, as no molecules have been identified, which are efficient in both cases. However, any compound affecting early events, such as excitotoxicity, should be given as soon as possible and preferably within the first hour post-stroke. Such early administration could be facilitated by improved medical care logistics and ambulance treatments, which have been shown feasible in several cases (Ebinger et al., 2014; Garber, 2007; Itrat et al., 2016; Saver et al., 2015) and is currently being tested in a clinical phase 3 study for NA-1 (See the FRONTIERS trial, NCT02315443, at ClinicalTrials.gov). In addition, it would be relevant to study the therapeutic time window in the rabbit small clot embolic stroke model, in which the efficacy of the only marketed drug against ischemic stroke, tissue plasminogen activator (tPA), has been correlated with its effects in humans (Lapchak, 2010). This model also allows studies of the effect of combinations of UCCB01-144 and tPA on efficacy, safety, and therapeutic dose- and time window (Lapchak, 2015; Lapchak and Araujo, 2007).

To examine the effect of biological variation, we here explored neuroprotective effects of UCCB01-144 using our well-established pMCAO model in mice of both sexes and at different ages. Whereas a statistically significant infarct reduction by 28% was seen in aged males, which was in similar range as the effect of UCCB01-144 in young males, no effect was seen in young female mice. We speculated that the lack of effect in female mice could be due to sex hormones or fluctuations of these, but neuroprotective effects of UCCB01-144

were not observed in female mice even after lowering estradiol levels. Potentially, the neuroprotective properties of estradiol (Liu and Yang, 2013), as well as those of progestin (De Nicola et al., 2013), could have masked or reduced the neuroprotective effects of UCCB01-144 in the two studies. In a broader perspective, women have a higher lifetime risk of suffering the consequences of a stroke than men, mainly because of a large increase in incidences and mortalities in older postmenopausal women. This has been ascribed to reduced levels of protective female sex hormones, but other physiological sex-differences and risk factors are in play too (Haast et al., 2012; Howe and McCullough, 2015). Thus, the translational issue of sex-specific neuroprotective effects of new drug substances is complex and probably better studied using aged female mice or other models mimicking peri- or postmenopausal stages that are more representative of the clinical situation in women (Haast et al., 2012; Howe and McCullough, 2015; Sohrabji et al., 2017).

Sex differences have been observed in other studies of neuroprotectants. Minocycline reduced infarct size in male mice but not in ovariectomized female mice, which has been explained by sex-dependent effects of the PARP-1 pathway (Li and McCullough, 2009; Sohrabji et al., 2017). Also, important for current study, female nNOS knockout mice showed larger infarct volumes after tMCAO than wild-type mice, which is the opposite effect of what is seen in male mice; and the nNOS inhibitor 7-nitroindozole was found to increase brain damage in female mice, but showed protection in male mice (McCullough et al., 2005). These data suggest that the neuronal NO pathway is only neurotoxic in male mice and actually protective in female mice, which could explain why we observe no effects of UCCB01-144 in our female pMCAO experiment as PSD-95 inhibitors are believed to act by decoupling NMDA receptor signaling downstream from PSD-95 and reduce nNOS activity (Aarts et al., 2002). However, Tat-NR2B9c at 3 nmol/g reduced infarct volumes in both male and female rats in the three-pial vessel occlusion model (Sun et al., 2008; Tymianski et al., 2011) either indicating that Tat-NR2B9c-mediated reduction in neuronal NO is not the only neuroprotective mechanism of this drug candidate (Bach, 2017) or that potential sex-dependent effects are not a general issue concerning PSD-95 as a target, but might relate to the specific compound, model, or species being studied. In any case, our results suggest that more pre-clinical studies are needed to elucidate sex-specific effects of PSD-95 inhibitors.

In conclusion, the dimeric compound UCCB01-144 and monomeric compound Tat-NR2B9c bound tandem PDZ1–2 domains of all four PSD-95-like MAGUKs (PDS-95, PSD-93, SAP-97, and SAP-102). The binding affinities were 300-1,600 fold higher for UCCB01-144 compared to those of Tat-NR2B9c, which correlated with higher efficiency with which UCCB01-144 pulled down MAGUKs from a complex mixture of brain lysate proteins. Mechanistically, we found that UCCB01-144 interfered with signaling proteins downstream of the nNOS/PSD-95/NMDA receptor complex as it decreased nNOS expression and increased the levels of phosphorylated (active) ERK1/2 6 h after pMCAO. The enhanced in vitro affinity of UCCB01-144 translated to improved in vivo efficiency in protecting rodents from ischemic brain damage compared with that of Tat-NR2B9c. In the pMCAO model, 3 or 9 nmol/g UCCB01-144 resulted in a 37% reduction of infarct volume, whereas Tat-NR2B9c was only effective at 9 nmol/g (infarct volume reduction by 32%). At 30 nmol/g, UCCB01-144 did not show neuroprotective properties, but also no severe cardiovascular side effects were observed in non-ischemic mice. In contrast, administration of 30 nmol/g Tat-NR2B9c was associated with death of almost all ischemic mice and with a severe and prolonged drop in HR of non-ischemic mice. Furthermore, 3 nmol/g UCCB01-144 reduced infarct size by 31% in tMCAO rats, whereas only a lower, statistical insignificant trend towards neuroprotection was detected for Tat-NR2B9c, and 9 nmol/g UCCB01-144 reduced infarct size by 28% in the pMCAO model using aged male mice. Overall, UCCB01-144 showed neuroprotective effects in rodents under various conditions and simultaneously had an apparently better cardiovascular safety profile than Tat-NR2B9c.

UCCB01-144 was not neuroprotective in young female mice or after the time of dosing was delayed from 30 to 60 min post-ischemia in young male mice, which are issues that should be studied further. Still, the obtained data indicate that UCCB01-144 is a potent PSD-95-PDZ1–2 inhibitor with neuroprotective properties that can be utilized in a broad range of conditions with a particular therapeutic potential in ischemic stroke.

Funding sources

This work was supported by The Simon Fougner Hartmanns Family Foundation (KLL), Danish Research Council (Grant 09-069636 for AB and 4183-00033 for KLL), Lundbeck Foundation (Grant R54-A5539 for KLL and R190-2014-3710 for AB), Hørslev Foundation (BHC), the Danish National Research Foundation (Grant PUMPKIN DNRF85 for KLH), and Wellcome Trust (KS, AB). During data analysis and preparation of this manuscript, MVK was supported by the UK Dementia Research Institute at Imperial College London. The funding sources had no involvement in the study design; collection, analysis or interpretation of data; or writing or submission of this article.

Acknowledgement

Prof. Michael Gajhede (University of Copenhagen, Denmark) and Prof. Per Jemth (Uppsala University, Sweden) are acknowledged for providing PDZ1–2 of PSD-93 and SAP-97, respectively.

Author contributions

All authors, i.e. AB, BHC, LKK, MGA, DGE, PBLH, HH, MH, DÖ, EJT, MVK, SGNG, KLH, FFJ, KLL, KS, have designed studies and interpreted results. AB, BHC, LKK, MGA, DGE, PBLH, HH, MH, DÖ, EJT, KLH, and KLL have performed experiments. The manuscript was written by AB, BHC, KLL and KS with input from remaining authors. All authors have approved the submission of the manuscript.

Conflicts of interest

AB and KS are founders and shareholders of Avilex Pharma pursuing the development of PSD-95 inhibitors to target unmet medical needs, including stroke. SGNG was a founder and shareholder of Synome Ltd. Remaining authors declares that they have no conflict of interest.

Appendix A. Supplementary data

Supplementary data related to this article can be found at…

References

Aarts, M., Liu, Y., Liu, L., Besshoh, S., Arundine, M., Gurd, J. W., Wang, Y.T., Salter, M.W., Tymianski, M., 2002. Treatment of ischemic brain damage by perturbing NMDA receptor-PSD-95 protein interactions. Science 298, 846-850.

Andersen, H., Jaff, M.G., Hogh, D., Vanhoutte, P., Hansen, P.B., 2011. Adenosine elicits an eNOS-independent reduction in arterial blood pressure in conscious mice that involves adenosine A(2A) receptors. Acta Physiol. 203, 197-207.

Atif, F., Yousuf, S., Sayeed, I., Ishrat, T., Hua, F., Stein, D.G., 2013. Combination treatment with progesterone and vitamin D hormone is more effective than monotherapy in ischemic stroke: The role of BDNF/TrkB/Erk1/2 signaling in neuroprotection. Neuropharmacology 67, 78-87.

Bach, A., 2017. Targeting oxidative stress in stroke. In: Lapchak, P.A, Zhang, J., (Eds), Neuroprotective Therapy for Stroke and Ischemic Disease. Springer International Publishing, pp. 203-250.

Bach, A., Chi, C.N., Olsen, T. B., Pedersen, S.W., Røder, M.U., Pang, G.F., Clausen, R.P., Jemth, P., Strømgaard, K., 2008. Modified peptides as potent inhibitors of the postsynaptic density-95/*N*-methyl-D-aspartate receptor interaction. J. Med. Chem. 51, 6450-6459.

Bach, A., Chi, C.N., Pang, G.F., Olsen, L., Kristensen, A.S., Jemth, P., Strømgaard, K., 2009. Design and synthesis of highly potent and plasma-stable dimeric inhibitors of the PSD-95-NMDA receptor interaction. Angew. Chem. Int. Ed. 48, 9685-9689.

Bach, A., Clausen, B.H., Møller, M., Vestergaard, B., Chi, C.N., Round, A., Sørensen, P.L., Nissen, K.B., Kastrup, J.S., Gajhede, M., Jemth, P., Kristensen, A.S., Lundström, P., Lambertsen, K.L., Strømgaard, K., 2012. A high-affinity, dimeric inhibitor of PSD-95 bivalently interacts with PDZ1-2 and protects against ischemic brain damage. Proc. Natl. Acad. Sci. U.S.A. 109, 3317-3322.

Ballarin, B., Tymianski, M., 2018. Discovery and development of NA-1 for the treatment of acute ischemic stroke. Acta Pharmacol. Sin. 39, 661-668.

Bell, K.F., Bent, R.J., Meese-Tamuri, S., Ali, A., Forder, J.P., Aarts, M.M., 2013. Calmodulin kinase IV-dependent CREB activation is required for neuroprotection via NMDA receptor-PSD95 disruption. J. Neurochem. 126, 274-287.

Bonfils, P.K., Reith, J., Hasseldam, H., Johansen, F.F., 2006. Estimation of the hypothermic component in neuroprotection provided by cannabinoids following cerebral ischemia. Neurochem. Int. 49, 508-518.

Bottger, P., Glerup, S., Gesslein, B., Illarionova, N.B., Isaksen, T.J., Heuck, A., Clausen, B.H., Fuchtbauer, E.M., Gramsbergen, J.B., Gunnarson, E., Aperia, A., Lauritzen, M., Lambertsen, K.L., Nissen, P., Lykke-Hartmann, K., 2016. Glutamate-system defects behind psychiatric manifestations in a familial hemiplegic migraine type 2 disease-mutation mouse model. Sci. Rep. 6, 22047.

Bratane, B.T., Cui, H., Cook, D.J., Bouley, J., Tymianski, M., Fisher, M., 2011. Neuroprotection by freezing ischemic penumbra evolution without cerebral blood flow augmentation with a postsynaptic density-95 protein inhibitor. Stroke 42, 3265-3270.

Carlisle, H.J., Fink, A.E., Grant, S.G., O'Dell, T.J., 2008. Opposing effects of PSD-93 and PSD-95 on long-term potentiation and spike timing-dependent plasticity. J. Physiol. 586, 5885-5900.

Carmichael, S.T., 2005. Rodent models of focal stroke: size, mechanism, and purpose. NeuroRx 2, 396-409.

Chi, C.N., Bach, A., Engström, A., Strømgaard, K., Lundström, P., Ferguson, N., Jemth, P., 2011. Biophysical characterization of the complex between human papillomavirus E6 protein and synapse-associated protein 97. J. Biol. Chem. 286, 3597-3606.

Christopherson, K.S., Hillier, B.J., Lim, W.A., Bredt, D.S., 1999. PSD-95 assembles a ternary complex with the *N*-methyl-D-aspartic acid receptor and a bivalent neuronal NO synthase PDZ domain. J. Biol. Chem. 274, 27467-27473.

Clausen, B.H., Degn, M., Sivasaravanaparan, M., Fogtmann, T., Andersen, M.G., Trojanowsky, M.D., Gao, H., Hvidsten, S., Baun, C., Deierborg, T., Finsen, B., Kristensen, B.W., Bak, S.T., Meyer, M., Lee, J., Nedospasov, S.A., Brambilla, R., Lambertsen, K.L., 2016. Conditional ablation of myeloid TNF increases lesion volume after experimental stroke in mice, possibly via altered ERK1/2 signaling. Sci. Rep. 6, 29291.

Cook, D.J., Teves, L., Tymianski, M., 2012a. A translational paradigm for the preclinical evaluation of the stroke neuroprotectant Tat-NR2B9c in gyrencephalic nonhuman primates. Sci. Transl. Med. 4, 154ra133.

Cook, D.J., Teves, L., Tymianski, M., 2012b. Treatment of stroke with a PSD-95 inhibitor in the gyrencephalic primate brain. Nature 483, 213-217.

Cui, H., Hayashi, A., Sun, H.S., Belmares, M.P., Cobey, C., Phan, T., Schweizer, J., Salter, M.W., Wang, Y.T., Tasker, R.A., Garman, D., Rabinowitz, J., Lu, P.S., Tymianski, M., 2007. PDZ protein interactions underlying NMDA receptor-mediated excitotoxicity and neuroprotection by PSD-95 inhibitors. J. Neurosci. 27, 9901-9915.

Cuthbert, P.C., Stanford, L.E., Coba, M.P., Ainge, J.A., Fink, A.E., Opazo, P., Delgado, J.Y., Komiyama, N.H., O'Dell, T.J., Grant, S.G., 2007. Synapse-associated protein 102/dlgh3 couples the NMDA receptor to specific plasticity pathways and learning strategies. J. Neurosci. 27, 2673-2682.

Dawson, V.L., Dawson, T.M., London, E.D., Bredt, D.S., Snyder, S.H., 1991. Nitric oxide mediates glutamate neurotoxicity in primary cortical cultures. Proc. Natl. Acad. Sci. U.S.A 88, 6368-6371.

De Nicola, A.F., Coronel, F., Garay, L.I., Gargiulo-Monachelli, G., Gonzalez Deniselle, M.C., Gonzalez, S.L., Labombarda, F., Meyer, M., Guennoun, R., Schumacher, M., 2013. Therapeutic effects of progesterone in animal models of neurological disorders. CNS Neurol. Disord. Drug Targets 12, 1205-1218.

Ebinger, M., Winter, B., Wendt, M., Weber, J.E., Waldschmidt, C., Rozanski, M., Kunz, A., Koch, P., Kellner, P.A., Gierhake, D., Villringer, K., Fiebach, J.B., Grittner, U., Hartmann, A., Mackert, B.M., Endres, M., Audebert, H.J., for the STEMO Consortium, 2014. Effect of the use of ambulance-based thrombolysis on time to thrombolysis in acute ischemic stroke: a randomized clinical trial. JAMA 311, 1622-1631.

Feng, W., Zhang, M., 2009. Organization and dynamics of PDZ-domain-related supramodules in the postsynaptic density. Nat. Rev. Neurosci. 10, 87-99.

Fiorentini, M., Bach, A., Strømgaard, K., Kastrup, J.S., Gajhede, M., 2013. Interaction partners of PSD-93 studied by X-ray crystallography and fluorescence polarization spectroscopy. Acta Cryst. D. 69, 587-594.

Frank, R.A.W., Komiyama, N.H., Ryan, T.J., Zhu, F., O'Dell, T.J., Grant, S.G.N., 2016. NMDA receptors are selectively partitioned into complexes and supercomplexes during synapse maturation. Nat. Commun. 7, 11264.

Garber, K., 2007. Stroke treatment–light at the end of the tunnel? Nat. Biotechnol. 25, 838-840.

Haast, R.A., Gustafson, D.R., Kiliaan, A.J., 2012. Sex differences in stroke. J. Cereb. Blood. Flow Metab. 32, 2100-2107.

Hansen, P.B., Hristovska, A., Wolff, H., Vanhoutte, P., Jensen, B.L., Bie, P., 2010. Uridine adenosine tetraphosphate affects contractility of mouse aorta and decreases blood pressure in conscious rats and mice. Acta Physiol 200, 171-179.

Hardingham, G.E., 2006. Pro-survival signalling from the NMDA receptor. Biochem. Soc. Trans. 34, 936-938.

Haugaard-Kedström, L.M., Fernandes, E.F.A., Strømgaard, K., 2017. Targeting PSD-95 as a Novel Approach in the Treatment of Stroke. In: Lapchak, P.A., Zhang, J.H., (Eds), Neuroprotective Therapy for Stroke and Ischemic Disease. Springer International Publishing, Cham, pp. 157-184.

Hill, M.D., Martin, R.H., Mikulis, D., Wong, J.H., Silver, F.L., Terbrugge, K.G., Milot, G., Clark, W.M., Macdonald, R.L., Kelly, M.E., Boulton, M., Fleetwood, I., McDougall, C., Gunnarsson, T., Chow, M., Lum, C., Dodd, R., Poublanc, J., Krings, T., Demchuk, A.M., Goyal, M., Anderson, R., Bishop, J., Garman, D., Tymianski, M., for the ENACT trial investigators, 2012. Safety and efficacy of NA-1 in patients with iatrogenic stroke after endovascular aneurysm repair (ENACT): a phase 2, randomised, double-blind, placebo-controlled trial. Lancet Neurol. 11, 942-950.

Howe, M.D., McCullough, L.D., 2015. Prevention and management of stroke in women. Expert. Rev. Cardiovasc. Ther. 13, 403-415.

Hu, B.R., Liu, C.L., Park, D.J., 2000. Alteration of MAP kinase pathways after transient forebrain ischemia. J. Cereb. Blood Flow Metab. 20, 1089-1095.

Huang, Z., Huang, P.L., Panahian, N., Dalkara, T., Fishman, M.C., Moskowitz, M.A., 1994. Effects of cerebral ischemia in mice deficient in neuronal nitric oxide synthase. Science 265, 1883-1885.

Itrat, A., Taqui, A., Cerejo, R., Briggs, F., Cho, S.M., Organek, N., Reimer, A.P., Winners, S., Rasmussen, P., Hussain, M.S., Uchino, K., for the Cleveland Pre-Hospital Acute Stroke Treatment (PHAST) Group, 2016. Telemedicine in prehospital stroke evaluation and thrombolysis: Taking stroke treatment to the Doorstep. JAMA Neurol. 73, 162-168.

Jeppsson, S., Gershagen, S., Johansson, E.D., Rannevik, G., 1982. Plasma levels of medroxyprogesterone acetate (MPA), sex-hormone binding globulin, gonadal steroids, gonadotrophins and prolactin in women during long-term use of depo-MPA (Depo-Provera) as a contraceptive agent. Acta Endocrinol 99, 339-343.

Kleinschnitz, C., Mencl, S., Kleikers, P.W.M., Schuhmann, M.K., Lopez, M.G., Casas, A.I., Surun, B., Reif, A., Schmidt, H.H.H.W., 2016. NOS knockout or inhibition but not disrupting PSD-95-NOS interaction protect against ischemic brain damage. J. Cereb. Blood Flow Metab. 36, 1508-1512.

Kucharz, K., Rasmussen, I.S., Bach, A., Strømgaard, K., Lauritzen, M., 2017. PSD-95 uncoupling from NMDA receptors by Tat-*N*-dimer ameliorates neuronal depolarization in cortical spreading depression. J. Cereb. Blood Flow Metab. 37, 1820-1828.

Lai, T.W., Zhang, S., Wang, Y.T., 2014. Excitotoxicity and stroke: identifying novel targets for neuroprotection. Prog. Neurobiol. 115, 157-188.

Lambertsen, K.L., Gregersen, R., Drojdahl, N., Owens, T., Finsen, B., 2001. A specific and sensitive method for visualization of tumor necrosis factor in the murine central nervous system. Brain Res. Brain Res. Protoc. 7, 175-191.

Lapchak, P.A., 2010. Translational stroke research using a rabbit embolic stroke model: A correlative analysis hypothesis for novel therapy development. Transl. Stroke Res. 1, 96-107.

Lapchak, P.A., 2015. A cost-effective rabbit embolic stroke bioassay: insight into the development of acute ischemic stroke therapy. Transl. Stroke Res. 6, 99-103.

Lapchak, P.A., Araujo, D.M., 2007. Advances in ischemic stroke treatment: neuroprotective and combination therapies. Expert Opin. Emerg. Drugs 12, 97-112.

Laursen, S.B., Finsen, S., Marcussen, N., Quaggin, S.E., Hansen, P.B.L., Dimke, H., 2018. Endothelial mineralocorticoid receptor ablation does not alter blood pressure, kidney function or renal vessel contractility. PLoS One 13, e0193032.

Li, J., McCullough, L.D., 2009. Sex differences in minocycline-induced neuroprotection after experimental stroke. J. Cereb. Blood Flow Metab. 29, 670-674.

Lim, I. A., Hall, D. D., Hell, J. W., 2002. Selectivity and promiscuity of the first and second PDZ domains of PSD-95 and synapse-associated protein 102. J. Biol. Chem. 277, 21697-21711.

Liu, R., Tang, J.C., Pan, M.X., Zhuang, Y., Zhang, Y., Liao, H.B., Zhao, D., Lei, Y., Lei, R.X., Wang, S., Liu, A.C., Qin, X.P., Chen, J., Zhang, Z.F., Wan, Q., 2018. ERK 1/2 activation mediates the neuroprotective effect of BpV(pic) in focal cerebral ischemia-reperfusion injury. Neurochem. Res. doi: 10.1007/s11064-018-2558-z (*in press*).

Liu, R., Yang, S.H., 2013. Window of opportunity: estrogen as a treatment for ischemic stroke. Brain Res. 1514, 83-90.

Longa, E.Z., Weinstein, P.R., Carlson, S., Cummins, R., 1989. Reversible middle cerebral-artery occlusion without craniectomy in rats. Stroke 20, 84-91.

McCullough, L.D., Zeng, Z., Blizzard, K.K., Debchoudhury, I., Hurn, P.D., 2005. Ischemic nitric oxide and poly (ADP-ribose) polymerase-1 in cerebral ischemia: male toxicity, female protection. J. Cereb. Blood Flow Metab. 25, 502-512.

Migaud, M., Charlesworth, P., Dempster, M., Webster, L.C., Watabe, A.M., Makhinson, M., He, Y., Ramsay, M. F., Morris, R.G., Morrison, J.H., O'Dell, T.J., Grant, S.G., 1998. Enhanced long-term potentiation and impaired learning in mice with mutant postsynaptic density-95 protein. Nature 396, 433-439.

Milstein, M.L., Musa, H., Balbuena, D.P., Anumonwo, J.M., Auerbach, D.S., Furspan, P.B., Hou, L., Hu, B., Schumacher, S.M., Vaidyanathan, R., Martens, J.R., Jalife, J., 2012. Dynamic reciprocity of sodium and potassium channel expression in a macromolecular complex controls cardiac excitability and arrhythmia. Proc. Natl. Acad. Sci. U.S.A 109, E2134-2143.

Tymianski, M., Garman, J.D., 2011. Co-administration of an agent linked to an internalization peptide with an anti-inflammatory. US 8,080,518 B2.

Sattler, R., Xiong, Z., Lu, W.Y., Hafner, M., MacDonald, J.F., Tymianski, M., 1999. Specific coupling of NMDA receptor activation to nitric oxide neurotoxicity by PSD-95 protein. Science 284, 1845-1848.

Saver, J.L., Starkman, S., Eckstein, M., Stratton, S.J., Pratt, F.D., Hamilton, S., Conwit, R., Liebeskind, D.S., Sung, G., Kramer, I., Moreau, G., Goldweber, R., Sanossian, N., for the FAST-MAG investigators and coordinators, 2015. Prehospital use of magnesium sulfate as neuroprotection in acute stroke. New Engl. J. Med. 372, 528-536.

Sawe, N., Steinberg, G., Zhao, H., 2008. Dual roles of the MAPK/ERK1/2 cell signaling pathway after stroke. J. Neurosci. Res. 86, 1659-1669.

Sohrabji, F., Park, M.J., Mahnke, A.H., 2017. Sex differences in stroke therapies. J. Neurosci. Res. 95, 681-691.

Soriano, F.X., Martel, M.A., Papadia, S., Vaslin, A., Baxter, P., Rickman, C., Forder, J., Tymianski, M., Duncan, R., Aarts, M., Clarke, P., Wyllie, D.J., Hardingham, G.E., 2008. Specific targeting of pro-death NMDA receptor signals with differing reliance on the NR2B PDZ ligand. J. Neurosci. 28, 10696-10710.

Stiffler, M.A., Chen, J.R., Grantcharova, V.P., Lei, Y., Fuchs, D., Allen, J.E., Zaslavskaia, L.A., MacBeath, G., 2007. PDZ domain binding selectivity is optimized across the mouse proteome. Science 317, 364-369.

Sun, H.S., Doucette, T.A., Liu, Y., Fang, Y., Teves, L., Aarts, M., Ryan, C.L., Bernard, P.B., Lau, A., Forder, J.P., Salter, M.W., Wang, Y.T., Tasker, R.A., Tymianski, M., 2008. Effectiveness of PSD95 inhibitors in permanent and transient focal ischemia in the rat. Stroke 39, 2544-2553.

Teves, L.M., Cui, H., Tymianski, M., 2016. Efficacy of the PSD95 inhibitor Tat-NR2B9c in mice requires dose translation between species. J. Cereb. Blood Flow Metab. 36, 555-561.

Vaidyanathan, R., Taffet, S. M., Vikstrom, K. L., Anumonwo, J. M., 2010. Regulation of cardiac inward rectifier potassium current (I(K1)) by synapse-associated protein-97. J. Biol. Chem. 285, 28000-28009.

Wu, D.C., Ye, W., Che, X.M., Yang, G.Y., 2000. Activation of mitogen-activated protein kinases after permanent cerebral artery occlusion in mouse brain. J. Cereb. Blood Flow Metab. 20, 1320-1330.

Zhang, F., Chen, J., 2008. Leptin protects hippocampal CA1 neurons against ischemic injury. J. Neurochem. 107, 578-587.

Zhou, L., Li, F., Xu, H.B., Luo, C.X., Wu, H.Y., Zhu, M.M., Lu, W., Ji, X., Zhou, Q.G., Zhu, D.Y., 2010. Treatment of cerebral ischemia by disrupting ischemia-induced interaction of nNOS with PSD-95. Nat. Med. 16, 1439-1443.

Figure legends

Fig. 1. Binding properties of PSD-95 inhibitors. (**A**) Chemical structures of the studied PSD-95 inhibitors. Capital letters indicate L-amino acids, except for 'N' (nitrogen) and 'O' (oxygen). (**B**) Affinity towards PDZ1–2 of PSD-93, SAP-97, and SAP-102 for UCCB01-144 (black boxes), UCCB01-125 (clear triangles), and Tat-NR2B9c (clear circles); and affinity of UCCB01-144 towards PDZ2 and PDZ3 of PSD-95 as measured by fluorescence polarization. Data are presented as the mean ± standard error of the mean (SEM) of ≥ 3 independent measurements. (**C**) Western blots illustrating pull-down of MAGUK proteins PSD-93, PSD-95, SAP-97 and SAP-102 by biotin-labeled UCCB01-144, UCCB01-125, and Tat-NR2B9c.

Fig. 2. Protein expression of nNOS (**A**, **B**), p-JNK1/2 (**C**, **D**), and p-ERK1/2 (**E**, **F**) in 6 and 48 h after induction of ischemia in mice (n = 6) treated with saline, Tat-NR2B9c, and UCCB01-144 ('144') was detected by western blotting. Data are presented as the mean fold change ± SEM relative to sham-operated animals (n = 3). Statistical significance of differences is indicated as follows: *p < 0.05; **p < 0.01; ***p < 0.001; one-way ANOVA followed by the Dunnett's multiple comparisons test.

Fig. 3. Neuroprotective properties of UCCB01-144 and Tat-NR2B9c in the pMCAO mouse model. (**A**–**C**) UCCB01-144 at concentrations of 1, 9, or 30 nmol/g and Tat-NR2B9c at a concentration of 9 nmol/g were administered to young adult male mice i.v. and 30 min post-surgery followed by a survival period of 47.5 h. Numbers of animals were as follows: (**A**) n = 17/16 (saline/UCCB01-144); (**B**) n = 12/18/18 (saline/Tat-NR2B9c/UCCB01-144); (**C**) n = 16/16 (Saline/UCCB01-144). (**D**) UCCB01-144 was administered to young adult male mice at 3 nmol/g 60 min post-surgery (i.v., survival period of 48 h). n = 11/12 (saline/UCCB01-144). (**E**) UCCB01-144 was administered to aged male mice at 9 nmol/g 30 min post-surgery (i.v., survival period of 24 h). n = 17/18 (saline/UCCB01-144). (**F**, **G**) UCCB01-144 was administered to young adult female mice (with or without prior Depo-provera treatment) at 9 nmol/g 30 min post-surgery (i.v., survival period of 24 h). Numbers of animals: (**F**) n = 20/23 (saline/UCCB01-144); (**G**) n = 17/18 (saline/UCCB01-144). (**A**–**G**) Data represent mean infarct volumes (mm^3) ± SEM. Statistical significance of differences is indicated as follows: *p < 0.05; (**A**, **C**–**G**) Student's two-tailed, unpaired t-test; (**B**) one-way ANOVA followed by the Tukey's multiple comparisons test.

Fig. 4. Neuroprotective properties of UCCB01-144 and Tat-NR2B9c in the tMCAO rat model. UCCB01-144 and Tat-NR2B9c were administered at a dose of 3 nmol/g (i.v., 60 min post-surgery, i.e. 30 min pre-reperfusion) followed by a survival period of 23 h. Numbers of animals: n = 9/10/11 (Saline/Tat-NR2B9c/UCCB01-144). Data represent total mean infarct volumes (mm^3) (**A**) or mean infarct areas (mm^2) across brain sections (**B**) both ± SEM. Statistical significance of differences is indicated as follows: *p < 0.05; one-way ANOVA followed by Tukey's multiple comparisons test.

Fig. 5. Mean arterial blood pressure (MABP) (**A**-**B**) and heart rate (HR) (**C**-**D**) measurements illustrated as continuous samplings every 5 min (in mmHg and beats/min, respectively) in wild-type non-ischemic mice. Both MABP and HR were measured over a time period of 4 h, with 2 h of baseline measurements followed by 2 h of sampling after administration of UCCB01-144 (**A**/**C**) or Tat-NR2B9c (**B**/**D**) at various doses (3, 9, or 30 nmol/g) at 120 min (indicated by line). Numbers of animals: (**A**/**C**), n = 4/5, 4/6, 4/5 (saline/UCCB01-144 at 3, 9, 30 nmol/g, respectively); (**B**/**D**), n = 4/3, 4/3, 4/3 (saline/Tat-NR2B9c at 3, 9, 30 nmol/g, respectively). (**A**–**D**) Data are shown as the mean ± SEM. Statistical significance of differences is indicated as follows: *p < 0.05, **p < 0.01;

two-way repeated measures (RM) ANOVA followed by the Bonferroni's post-test for multiple comparisons to control group.

Tables

Table 1. Affinities of the studied compounds towards PDZ domains of MAGUK proteins (K_i values in nM[a])

	PSD-95 (PDZ1–2)	PSD-93 (PDZ1–2)	SAP-97 (PDZ1–2)	SAP-102 (PDZ1–2)	PSD-95 (PDZ2)	PSD-95 (PDZ3)
UCCB01-AB144	4.6 ± 0.3[b]	6.5 ± 0.9	2.8 ± 0.5	1.2 ± 0.9	1,000 ± 30	87,000 ± 9,000
UCCB01-AB125	9.5 ± 0.3[b]	8.6 ± 0.4	5.9 ± 0.6	22 ± 1	1,000 ± 70[c]	50,000 ± 1,000[c]
Tat-NR2B9c	4,600 ± 300[b]	2,100 ± 100	2,700 ± 300	1,900 ± 70	4,400 ± 300[d]	No activity[d]

[a]Data are shown as mean ± SEM, n ≥ 3. Data from previous studies are indicated as follows: [b]Data from (Bach et al., 2012); [c]Data from (Bach et al., 2009); [d]Data from (Bach et al., 2008) (all other data are from current study)

Figure 1

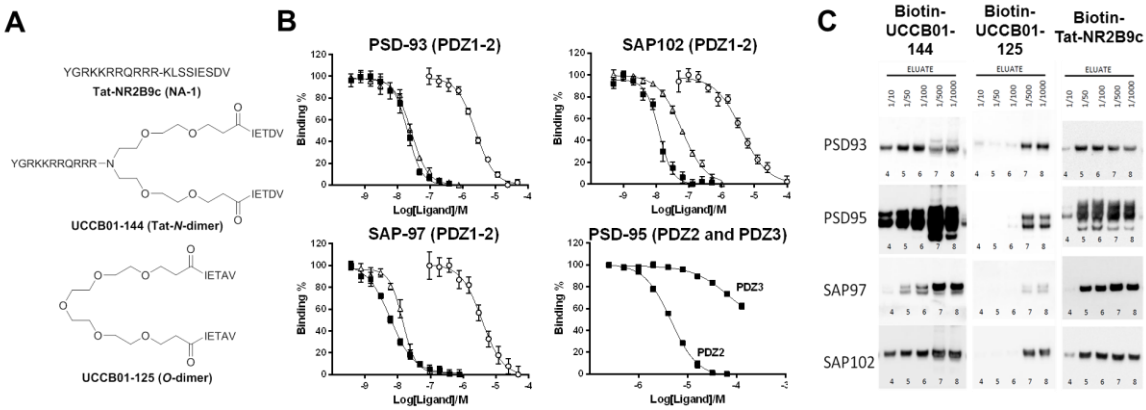
A
YGRKKRRQRRR-KLSSIESDV
Tat-NR2B9c (NA-1)
YGRKKRRQRRR
IETDV
IETDV
UCCB01-144 (Tat-N-dimer)
IETAV
IETAV
UCCB01-125 (O-dimer)
B
PSD-93 (PDZ1-2)
SAP102 (PDZ1-2)
SAP-97 (PDZ1-2)
PSD-95 (PDZ2 and PDZ3)
PDZ3
PDZ2
Binding %
Log[Ligand]/M
C
Biotin-UCCB01-144
Biotin-UCCB01-125
Biotin-Tat-NR2B9c
ELUATE
PSD93
PSD95
SAP97
SAP102

Figure 2

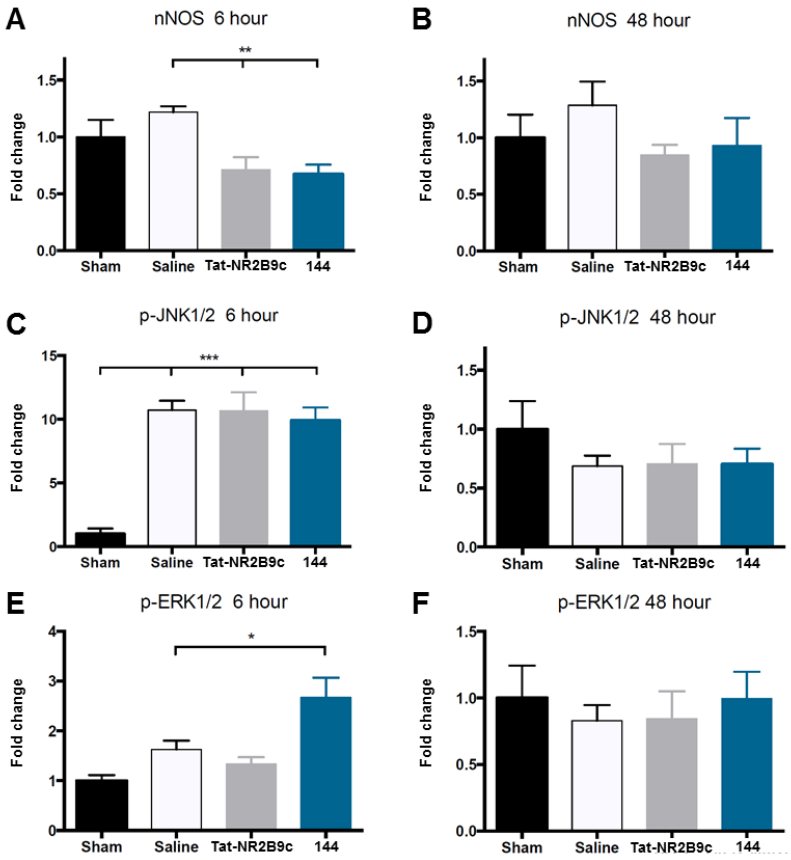
A
nNOS 6 hour
**
Fold change
1.5
1.0
0.5
0.0
Sham
Saline
Tat-NR2B9c
144
B
nNOS 48 hour
Fold change
1.5
1.0
0.5
0.0
Sham
Saline
Tat-NR2B9c
144
C
p-JNK1/2 6 hour
***
Fold change
15
10
5
0
Sham
Saline
Tat-NR2B9c
144
D
p-JNK1/2 48 hour
Fold change
1.5
1.0
0.5
0.0
Sham
Saline
Tat-NR2B9c
144
E
p-ERK1/2 6 hour
*
Fold change
4
3
2
1
0
Sham
Saline
Tat-NR2B9c
144
F
p-ERK1/2 48 hour
Fold change
1.5
1.0
0.5
0.0
Sham
Saline
Tat-NR2B9c
144

Figure 3

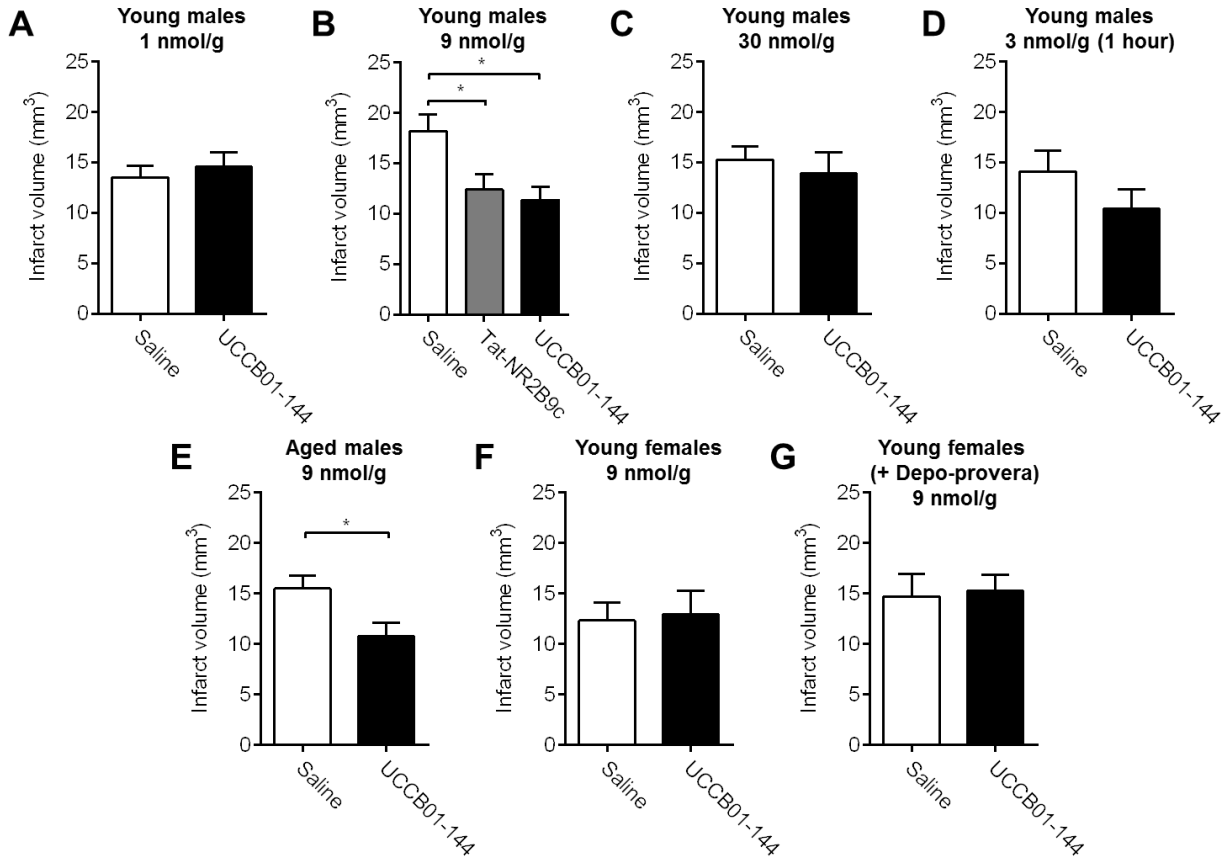
A
Young males
1 nmol/g
B
Young males
9 nmol/g
C
Young males
30 nmol/g
D
Young males
3 nmol/g (1 hour)
E
Aged males
9 nmol/g
F
Young females
9 nmol/g
G
Young females
(+ Depo-provera)
9 nmol/g
Infarct volume (mm3)
0
5
10
15
20
25
*
Saline
Tat-NR2B9c
UCCB01-144

Figure 4

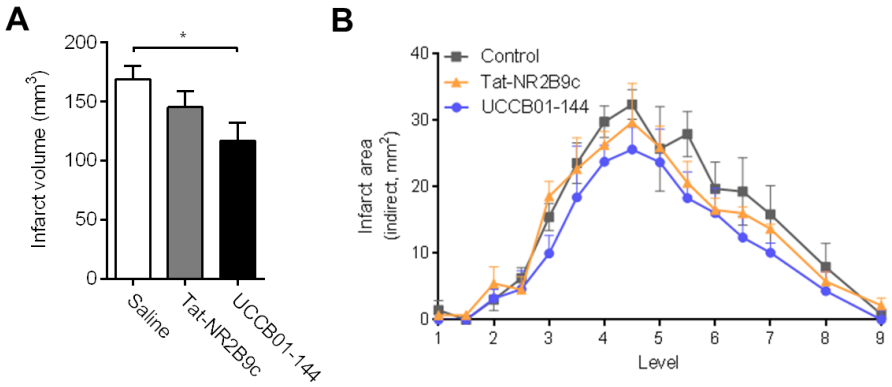
A
B
Infarct volume (mm3)
200
150
100
50
0
*
Saline
Tat-NR2B9c
UCCB01-144
Infarct area (indirect, mm2)
40
30
20
10
0
Control
Tat-NR2B9c
UCCB01-144
1
2
3
4
5
6
7
8
9
Level

Figure 5

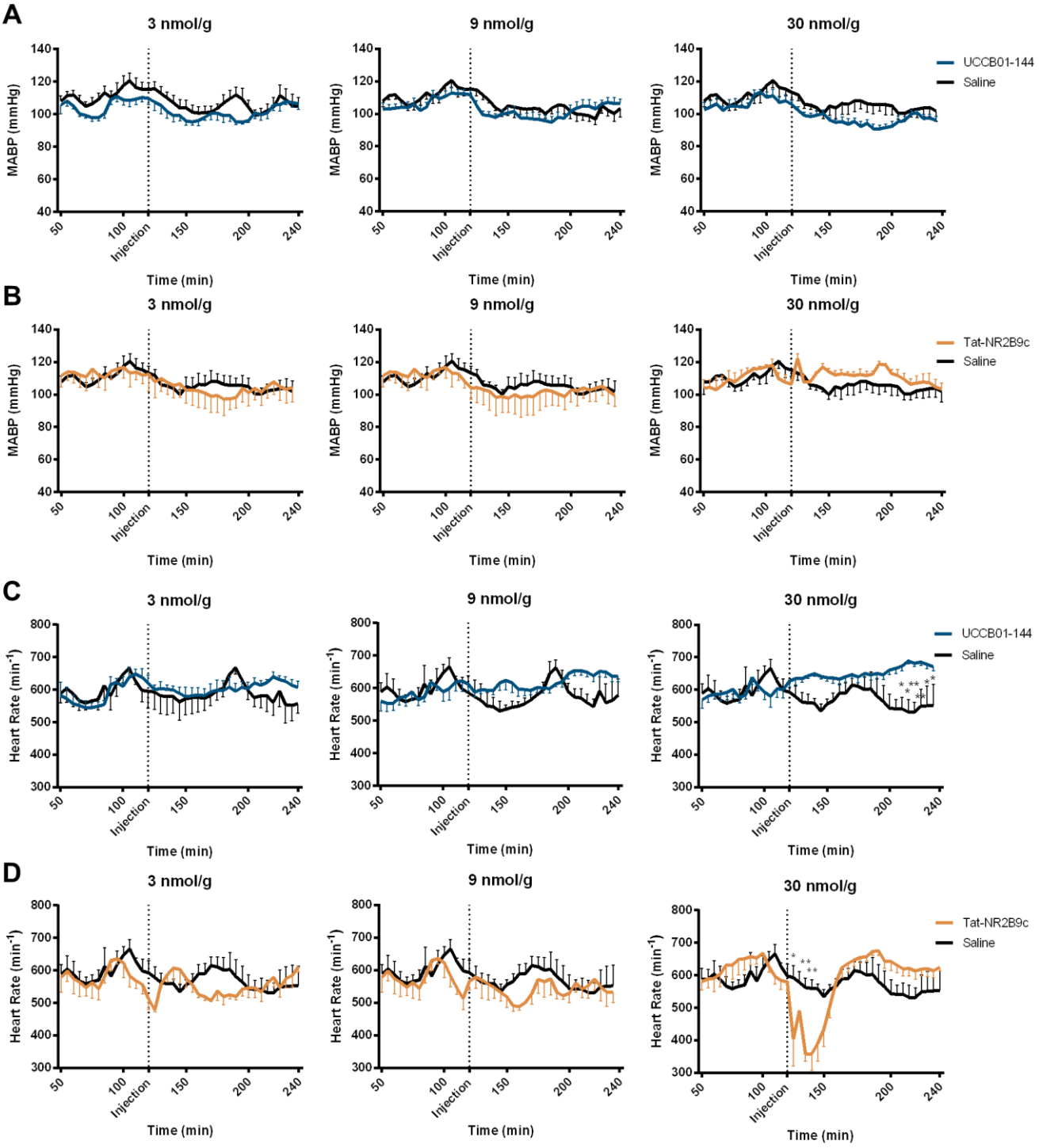
A
3 nmol/g
9 nmol/g
30 nmol/g
MABP (mmHg)
Time (min)
Injection
UCCB01-144
Saline
B
3 nmol/g
9 nmol/g
30 nmol/g
MABP (mmHg)
Time (min)
Injection
Tat-NR2B9c
Saline
C
3 nmol/g
9 nmol/g
30 nmol/g
Heart Rate (min-1)
Time (min)
Injection
UCCB01-144
Saline
D
3 nmol/g
9 nmol/g
30 nmol/g
Heart Rate (min-1)
Time (min)
Injection
Tat-NR2B9c
Saline

Supplementary Material

Click here to download Supplementary Material: Bach2018Neuropharmacology_AppA_Supplementary Data_v1.pdf

Manuscript w tracked changes

Click here to download Supplementary Material: Bach2018Neuropharmacology_Manus_v8_tracked.docx